

High-speed ellipsometer

201506011

PD Hsieh Yi-Da

Introduction

Ellipsometry is generally defined as the task of measuring the state of polarization of a light wave. A general ellipsometer configuration consists of six parts: the light source, polarizer, compensator, sample, analyzer and the detector. In conventional method, two general configurations are used for measurement, null and photometric ellipsometer. The null ellipsometer is to minimize or “nulled” the light intensity at the detector by adjusting the angle of the polarizer. In photometric ellipsometry, the analyzer is rotated and the light intensity is measured at different rotational angles of the analyzer. The measurement speeds are limited by the rotation speed of polarizer and analyzer [1].

Determination of retardation parameters of multiple-order wave plate using a phase-sensitive heterodyne ellipsometer [2]

A multiple-order wave plate (MWP) can adjust the polarization state of light waves, and changing its thickness or using a different wavelength of light wave achieves this. Furthermore, the polarization state can also be adjusted by tilting the wave plate such that the laser beam is obliquely incident onto the wave plate. In this study, we set up a phase-sensitive optical heterodyne ellipsometer to measure the phase retardation of the P and S waves for measurement of the retardation parameters.

Experiment setup & method:

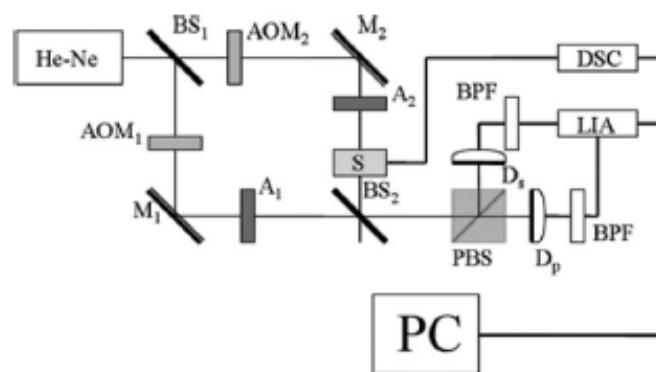


Fig. 1. Experimental setup: BS1, BS2: beam splitters, AOM1, AOM2: acousto-optic modulators, M1, M2: mirrors, A1, A2: analyzers, S: test sample on rotation stage, PBS: polarization beam splitter, D_p, D_s: photo detectors, BPF: band-pass filter, LIA: lock-in amplifier, DSC: digital stepping controller, PC: personal computer.

A linearly polarized laser beam is incident into the Mach-Zehnder interferometer such that the P₁ and S₁ waves are in the reference channel whereas the P₂ and S₂ waves are in the signal channel.

The laser beam is oblique incident onto the surface of MWP in two conditions where the oblique incident angle in x-z plane and y-z plane as shown in Fig. 2.

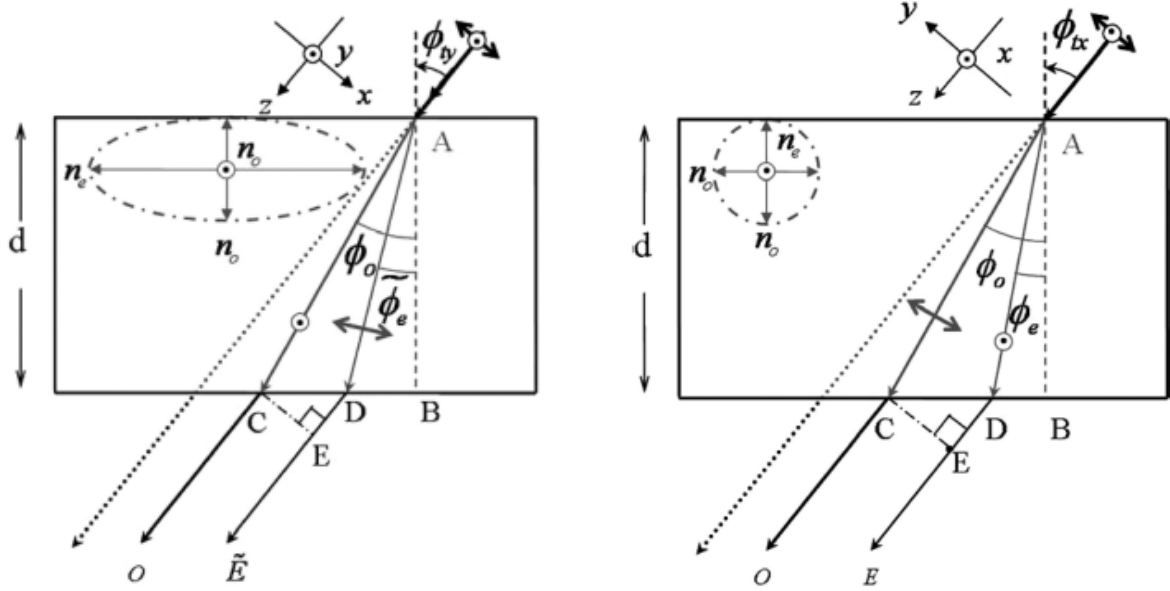


Fig. 2. Schematic diagram of the oblique incident angle of MWP.

The phase difference δ_{ty} and δ_{tx} from δ_0 becomes:

$$\delta_{ty} - \delta_0 = (\delta_s - \delta_p) - (\delta_{s_0} - \delta_{p_0}) = \frac{2\pi}{\lambda} d \left[\left(\sqrt{n_o^2 - \sin^2 \phi_{ty}} - \sqrt{n_e^2 - \frac{n_e^2}{n_o^2} \sin^2 \phi_{ty}} \right) - (n_o - n_e) \right]$$

and

$$\delta_{tx} - \delta_0 = (\delta_s - \delta_p) - (\delta_{s_0} - \delta_{p_0}) = \frac{2\pi}{\lambda} d \left[\left(\sqrt{n_o^2 - \sin^2 \phi_{tx}} - \sqrt{n_e^2 - \sin^2 \phi_{tx}} \right) - (n_o - n_e) \right]$$

For a linearly birefringent medium, the true phase retardation of the MWP is expressed by

$$\frac{2\pi}{\lambda} d(n_e - n_o) = 2m\pi + \Gamma.$$

However, the effect of multiple reflections needs to be considered at an oblique incidence. To reduce the multiple-reflection effect, δ_{ty} is subtracted from δ_{tx} at $\Phi_{ty} = \Phi_{tx} = \Phi_t$ and the common multiple reflection effects is therefore effectively cancelled. Thus,

$$\begin{aligned} (\delta_{ty} - \delta_{tx}) / (2m\pi + \Gamma) = & \left(\sqrt{n_e^2 - \sin^2 \phi_t} \right. \\ & \left. - \sqrt{n_e^2 - n_e^2 \sin^2 \phi_t / n_o^2} \right) / (n_e - n_o). \end{aligned}$$

Using the least square error fitting between the experimental data and this Eq. where the thickness of the MWP and the wavelength λ are given.

Result:

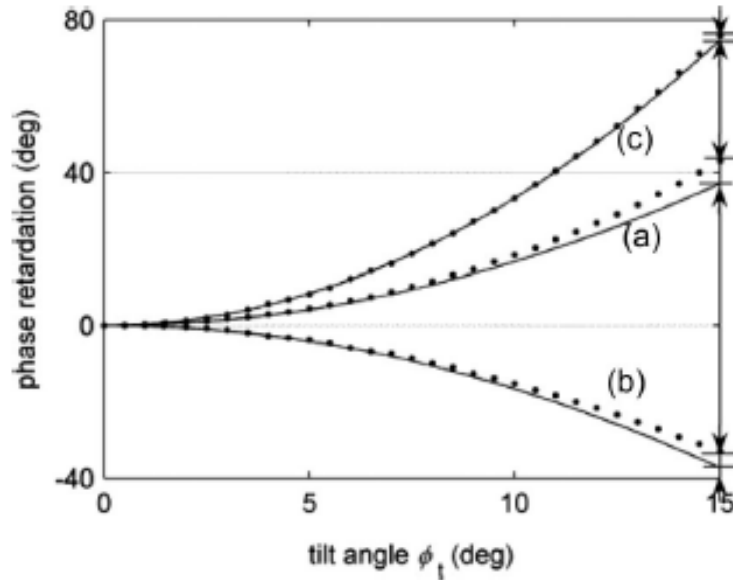


Fig. 2. Measured values versus tilt angle

Fig. 2 shows the experiment results, the value $n_e - n_o = 0.00908$ was calculated based on the experimentally calculated data for the order number $m = 7$ and the given thickness $d = 0.506$ mm of the antireflected coated QWP, and then $n_o = 1.54188$ and $n_e = 1.55096$ were obtained by the best curve-fitting of Fig. 8(c). When these results are compared with the reference data for the quartz wave plate ($n_o = 1.5427$, $n_e = 1.5518$), the percentage error is 0.05%.

High speed interferometric ellipsometer[3]

For the heterodyne measurement of ellipsometer, equal amplitude of two polarized heterodyne signals is required. In this paper, the author proposes a high-speed interferometric ellipsometer not only able to measure ellipsometric parameters in real time but also to relax the requirement of equal amplitude of two polarized heterodyne signals.

Experiment setup & method:

The optical setup is shown in Fig. 3. A frequency-stabilized linearly polarized laser beam is used in this polarized common-path heterodyne interferometer that three heterodyne signals including P polarized heterodyne signal, S polarized heterodyne signal, and also their differential one, are measured simultaneously. All these heterodyne signals are modulated at the same carrier frequency. Among them, the P polarized ($P_1 + P_2$) and S polarized ($S_1 + S_2$) heterodyne signals are phase-modulated.

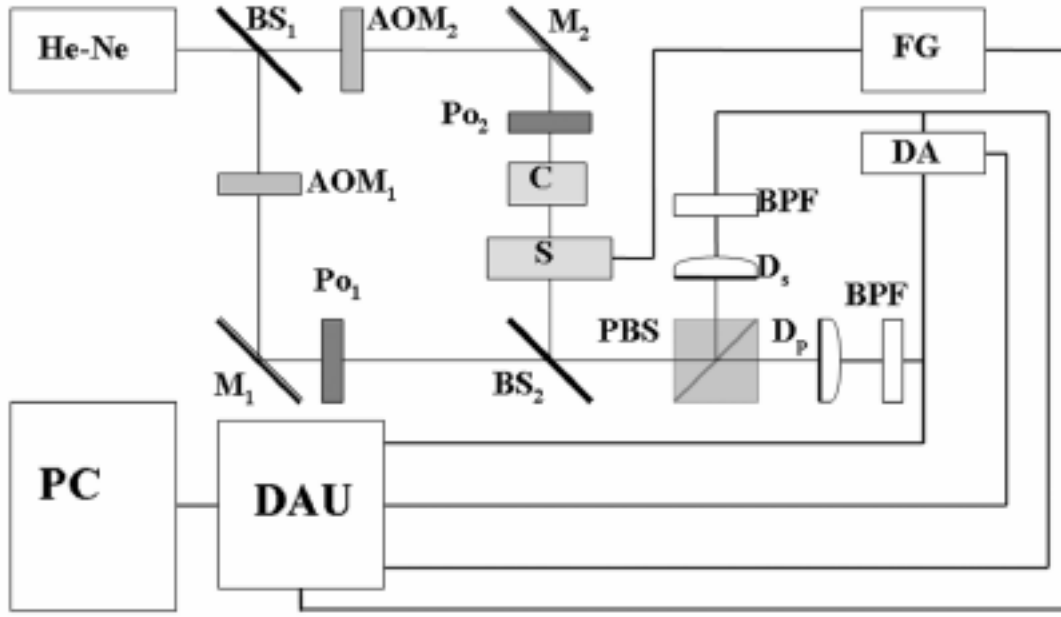


Fig. 3. The optical setup.

The polarized heterodyne signals at photo-detectors D_p and D_s can be expressed by

$$I_p(\delta\omega t) = A_{p1}^2 + A_{p2}^2 + 2A_{p1}A_{p2} \cos[\delta\omega t + \delta\phi_p],$$

$$I_s(\delta\omega t) = A_{s1}^2 + A_{s2}^2 + 2A_{s1}A_{s2} \cos[\delta\omega t + \delta\phi_s],$$

If only AC terms are considered,

$$I_p(\delta\omega t) = 2A_{p1}A_{p2} \cos[\delta\omega t + \delta\phi_p],$$

$$I_s(\delta\omega t) = 2A_{s1}A_{s2} \cos[\delta\omega t + \delta\phi_s],$$

set

$$\alpha = \delta\omega t + \frac{\delta\phi_s + \delta\phi_p}{2}, \quad \beta = \frac{\delta\phi_s - \delta\phi_p}{2}, \quad \kappa_p = 2A_{p1}A_{p2}, \quad \text{and} \quad \kappa_s = 2A_{s1}A_{s2}$$

then

$$I_p(\delta\omega t) \equiv \kappa_p \cos[\alpha - \beta],$$

$$I_s(\delta\omega t) \equiv \kappa_s \cos[\alpha + \beta],$$

Let and, $(\kappa_s - \kappa_p)\cos\beta = \cos\gamma$ and $(\kappa_s + \kappa_p)\sin\beta = \sin\gamma$, then the output signal, from DA in Fig. 3 can be expressed by

$$\begin{aligned}
 I_{Diff}(\delta\omega t) &= I_s(\delta\omega t) - I_p(\delta\omega t) \\
 &= (\kappa_s - \kappa_p)\cos\beta\cos\alpha - (\kappa_s + \kappa_p)\sin\beta\sin\alpha \\
 &= \cos\gamma\cos\alpha - \sin\gamma\sin\alpha = \sqrt{\kappa_s^2 + \kappa_p^2 - 2\kappa_s\kappa_p\cos(\delta\phi_s - \delta\phi_p)}\cos(\alpha + \gamma) \\
 &= \kappa_{Diff}\cos(\alpha + \gamma)
 \end{aligned}$$

The κ_{Diff} is the amplitude of $I_{Diff}(\delta\omega t)$ which belongs to an amplitude-modulated signal of the beat frequency $\delta\omega$. Thus,

$$\begin{aligned}
 \Delta &= \cos^{-1}\left[\frac{\kappa_p^2 + \kappa_s^2 - \kappa_{Diff}^2}{2\kappa_p\kappa_s}\right], \\
 \psi &= \tan^{-1}\left(\frac{\kappa_s}{\kappa_p}\right).
 \end{aligned}$$

Result:

Experimentally, a quarter wave plate (QWP) was tested and the experimental results are shown in Fig. 4 where the QWP was rotated along its normal axis during the measurement. Then the measured Δ becomes well agree with the measurement by using a lock-in amplifier (LIA) (Fig. 4 (f) solid line). Similarly, the same performance on noise resistance of phase is observed too. From these measured results, the validation of working principle of HSIE based on amplitude-sensitive detection method is demonstrated and proved experimentally.

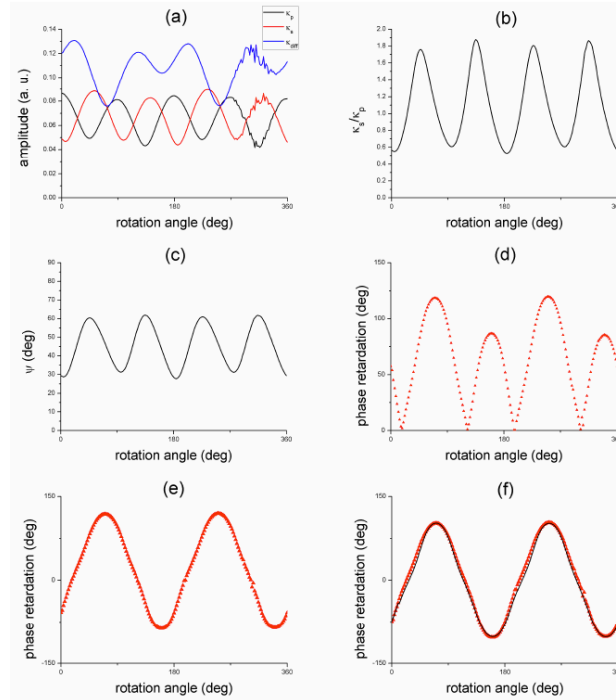


Fig. 4 Experimental results of QWP.

Meanwhile, in order to check the ability of real time measurement of HSIE, a homogeneous parallel aligned liquid crystal device (PALCD) was tested. It can be measured by measuring time-dependent phase retardation of PALCD which is controlled by an external applied voltage dynamically. Figure 3(a) shows the structure of LC molecule. When AC voltage is applied, the LC molecules between two Indium-Tin-Oxide (ITO) layers are symmetrically tilted as shown in Fig. 3(d).

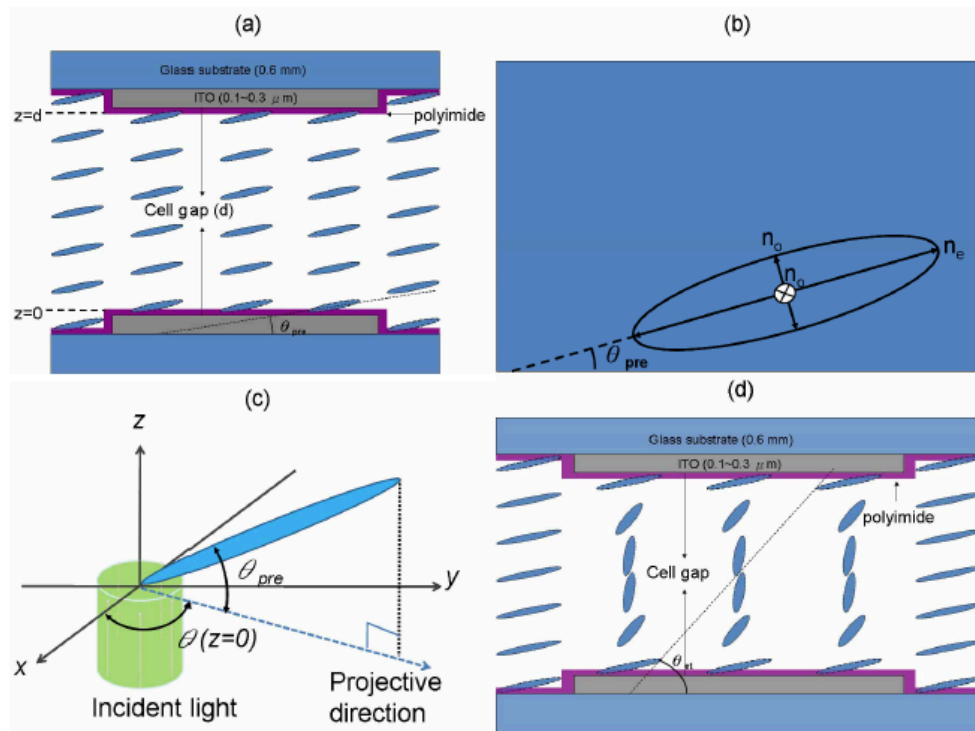


Fig. 5 The structure of LC molecule.

Figure 5 shows the response of phase retardation versus applied AC voltage. There is a plateau happened at small applied voltage and then drop rapidly until a smooth response is reached. The time response of Δ of PALCD versus applied square wave voltage at 1 KHz is shown in Fig. 6. It is obviously seen that the rise time and decay time are different and can be measured very precisely and dynamically. This result proves that the ability of HSIE on high-speed Δ measurement is applicable.

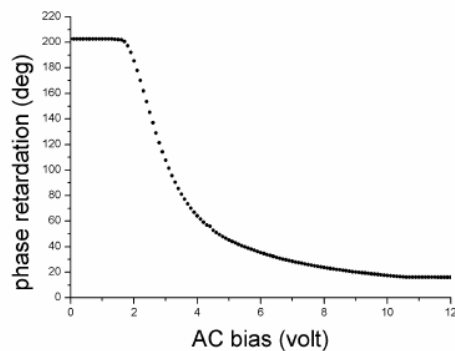


Fig. 5 Experimental results of phase retardation versus AC bias.

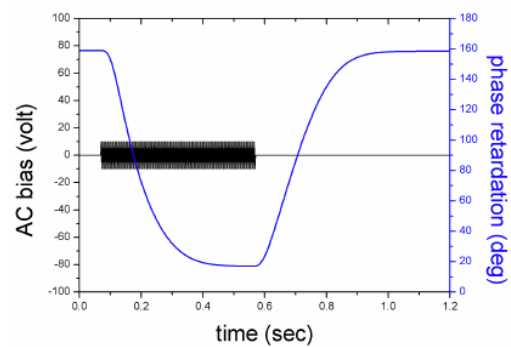


Fig. 6. The time response of Δ of PALCD.

Dual-frequency paired polarization phase shifting ellipsometer[4]

In this paper, the author combines the features of the phase shifting interferometer and common-path polarized heterodyne interferometric ellipsometer where the ellipsometric parameters of a specimen are measured accurately.

Experiment setup & method:

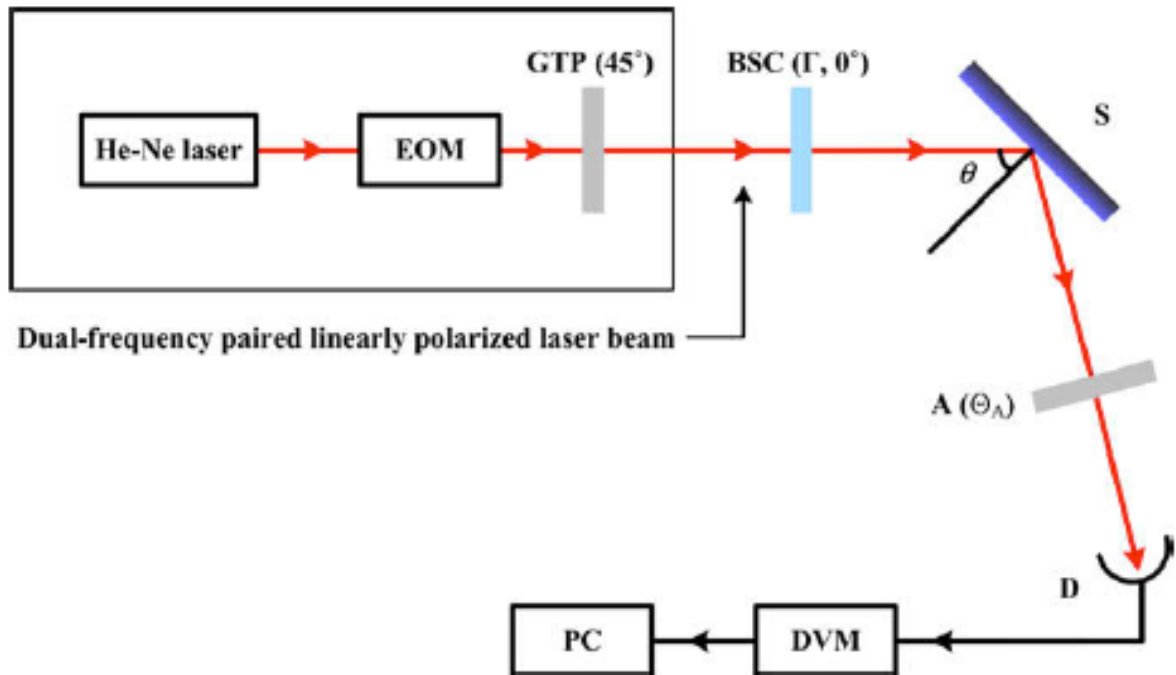


Fig. 7 The setup of DPPSE.

Figure. 7 shows the experiment setup of DPPSE. A dual-frequency linearly polarized laser beam is produced by using a frequency stabilized linearly polarized He-Ne laser beam integrated with an electro-optic modulator (EOM) that is driven at frequency ω . The Mueller matrices of BSC and analyzer are expressed as

$$\mathbf{M}_{\text{BSC}} = T_{\text{BSC}} \begin{pmatrix} 1 & 0 & 0 & 0 \\ 0 & 1 & 0 & 0 \\ 0 & 0 & \cos \Gamma & \sin \Gamma \\ 0 & 0 & -\sin \Gamma & \cos \Gamma \end{pmatrix},$$

$$\mathbf{M}_{\text{A}} = T_{\text{A}} \begin{pmatrix} 1 & \cos 2\theta_{\text{A}} & \sin 2\theta_{\text{A}} & 0 \\ \cos 2\theta_{\text{A}} & \cos^2 2\theta_{\text{A}} & \sin 2\theta_{\text{A}} \cos 2\theta_{\text{A}} & 0 \\ \sin 2\theta_{\text{A}} & \sin 2\theta_{\text{A}} \cos 2\theta_{\text{A}} & \sin^2 2\theta_{\text{A}} & 0 \\ 0 & 0 & 0 & 0 \end{pmatrix}.$$

T_{BSC} and T_{A} are the transmittance of BSC and analyzer, respectively; Γ is the phase retardation of BSC.

Hence, the intensity of the emerging beam can be described by

$$\tilde{I} = I_0 [1 - \cos 2\psi \cos 2\Theta_A + \sin 2\psi \cos(\Delta + \Gamma) \sin 2\Theta_A]$$

If Γ of BSC is adjusted at 0° and Θ_A is set either at 0° or 90° then,

$$\psi = \tan^{-1} \left(\tilde{I}_p / \tilde{I}_s \right)^{1/2}$$

Thus, Δ can be obtained by shifting the phase retardation Γ of BSC at 0° , 90° , 180° , and 270° sequentially.

$$\alpha = \frac{\tilde{I}_1 - \tilde{I}_3}{\tilde{I}_1 + \tilde{I}_3} = \sin 2\psi \cos \Delta,$$

$$\beta = \frac{\tilde{I}_4 - \tilde{I}_2}{\tilde{I}_4 + \tilde{I}_2} = \sin 2\psi \sin \Delta,$$

then Δ is calculated by

$$\Delta = \tan^{-1}(\beta/\alpha)$$

In order to demonstrate the capability of DPPSE able to measure the EP of a low absorbed material of which the phase retardation Δ is close to 0° or 180° for various incident angles, a bare silicon wafer was tested for the verification. The complex refractive index N of a bared silicon wafer is calculated in Table 2.

Table 1. Measured data of a bared silicon wafer at incident angle $\theta=80^\circ$.

Area	Ellipsometric parameters		Thickness
	ψ ($^\circ$)	Δ ($^\circ$)	T (nm)
#3: Measured	11.14	162.42	290.95
#3: Calibrated	10.83	162.23	290.16
#4: Measured	38.93	280.26	187.96
#4: Calibrated	38.30	280.06	189.20

A step wafer was also tested in order to demonstrate the capability of DPPSE to measure thin film thickness. The calibrated step wafer in which the silicon dioxide thin film was deposited on the silicon substrate was tested. Table 3 shows the results at different areas that present different thickness. The incident angle of laser beam was 70° in this experiment. The well agreement between measured and calibrated data clearly demonstrates the accuracy of DPPSE.

Table 2. The measurement of thickness of SiO₂ thin film.

	Ellipsometric parameters		Refractive index	
	ψ (°)	Δ (°)	n	k
Measured	10.62	0.59	3.95	0.015
Calculated	11.16	0.73	3.88	0.019

^a The calculated EP (ψ, Δ) is computed by using Matlab 7.0.1 program.

Reference

- [1] Ellipsometry, ALBORG UNIVERSITY, Ellipsometry PROJECT.
- [2] C. -H. Hsieh, *et. al.*, Appl. Opt. **46**: 5944 (2007)
- [3] C. -C. Tsai, *et., al.*, Opt. Express. **16**: 7778 (2008)
- [4] C. -J. Yu., *et., al.*, Opt. commun. **282**:1516 (2009)